EPSC Abstracts
Vol. 10, EPSC2015-24, 2015
European Planetary Science Congress 2015

A numerical method for true polar wander of a laterally heterogeneous planet

H. Hu , W. van der Wal and L.L.A.Vermeersen
Delft University of Technology, Netherlands (h.hu-1@tudelft.nl)

Abstract

The displacement of a celestial body's rotational axis with respect to its surface feature, or true polar wander (TPW) is studied in this paper and a numerical method is established which can deal with laterally heterogeneous models. This method is validated by comparing the numerical results with the analytical results which are developed based on normal mode theory. The results show good agreement. A further study of the TPW on Mars with a model which contains varying mantle viscosity is being conducted with the established numerical method.

1. Introduction

Analytically, the dynamics of polar wander is governed by two equations. Firstly, Liouville equation gives the general dynamics of a rotational body. When no external torque is applied, it reads $\frac{d}{dt}(\boldsymbol{I}\cdot\boldsymbol{\omega})+\boldsymbol{\omega}\times\boldsymbol{I}\cdot\boldsymbol{\omega}=0$, where $\boldsymbol{I}$ is the inertia tensor and $\boldsymbol{\omega}$ is the angular velocity vector. Both values are defined in a body fixed coordinate system. The analytical approach requires another equation which describes the moment of inertia $\boldsymbol{I}$. As the moment of inertia is perturbed by a geophysical process,the mass within the body redistributes and as the rotation axis changes, so the altered centrifugal force also deforms the rotational body. The total moment of Inertia attributable to such process is given by [1]

$$\boldsymbol{I}_{ij}(t) = I\delta_{ij} + \frac{k^T(t)a^5}{3G} * [\omega_i(t)\omega_j(t) - \frac{1}{3}\omega^2(t)] + [\delta(t) + k^L(t)] * C_{ij}(t) \quad (1)$$

Where I is the moment of inertia of the homogeneous spherical body, G is the gravitational constant. $k^T(t)$ and $k^L(t)$ are the degree 2 tidal love number and load love number respectively. C_{ij} represents the change in the moment of inertia without considering the dynamic deformation and it is this value that triggers the polar wander. The second and third term in Equation 1 stands for the changes which derive from the perturbed centrifugal force and from the mass redistribution induced by the triggering load respectively.
The analytical approach contains two major restrictions: First, the love numbers $k^T(t)$ and $k^L(t)$ can generally only be obtained for a homogeneous model. Secondly certain assumptions which simplify Equation 1 in the frequency domain are required so that it can be analytically solved together with the Liouville equation. However, these assumptions may not be true for other celestial bodies other than Earth. As a result, it is necessary to seek a numerical approach with which a general laterally heterogeneous planet can be studied.

2 Methodology

2.1 Numerical solutions of Liouville equation

First, we show that with the information about change in the moment of inertia, Liouville equation can be solved numerically with iterations. For a small enough time step, we assume that the change of moment of inertia varies linearly and by linear theory, Liouville equation leads to

$$m_1(t) = \frac{\Delta I_{13}(t)}{C-A} + \frac{C\Delta\ \dot{I}_{23}\ (t)}{\Omega(C-A)(C-B)} \quad (2a)$$

$$m_2(t) = \frac{\Delta I_{23}(t)}{C-B} + \frac{C\Delta\ \dot{I}_{13}\ (t)}{\Omega(C-A)(C-B)} \quad (2b)$$

with angular velocity defined as $\boldsymbol{\omega} = \Omega(m_1, m_2, 1 + m_3)$. In each step, the polar wander $m_i(t)$ is given an initial estimate and then the correspondent change of moment of inertia is computed from Equation 1. This value is then fed into Equation 2 to obtain the new $m_i(t)$ and the iteration continues until the result converges. The comparison between this numerical

method and the analytical one from [3] is shown in Figure 1.

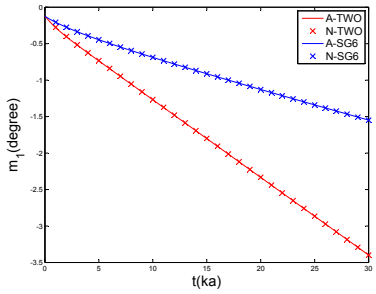

Figure 1: The polar wander path of two Earth models triggered by a point mass of 2×10^{19}kg placed at 45° colatitude in x-z plane. Lines shows the analytical(A) results and symbols represents the numerical (N) ones.

2.2 Finite element approach for change of moment of inertia

Next, we show that the change of moment of inertia can be numerically calculated instead of using Equation 1. [2] provides a finite element(FE) solution for calculating gravitationally self-consistent layered model by coupling the gravity term into the rheology equation through iterations. With information in the radius deformation, the change of moment of inertia for each layer can be calculated from

$$\Delta I_{ij,p} \simeq \int_S (\rho_{i+1} - \rho_i)(r_k r_k \delta_{ij} - r_i r_j) u_r dS \quad (3)$$

where ρ_i are densities of different layers and u_r is the radius displacement. When polar wander history is given and only the centrifugal force is considered for the laterally homogeneous model, the comparison between the analytical and FE results for calculating the change in moment of inertia is given in Figure 2.

For the theoretical non-zero components I_{11}, I_{22}, I_{33}, and I_{13}. The numerical result shows good correspondence with the analytical result. Theoretically, I_{12} and I_{23} should be zero. The results obtained from numerical methods have magnitudes which are about 4th order lower than the other four. These values represent the numerical errors which are estimated be around 0.1 %.

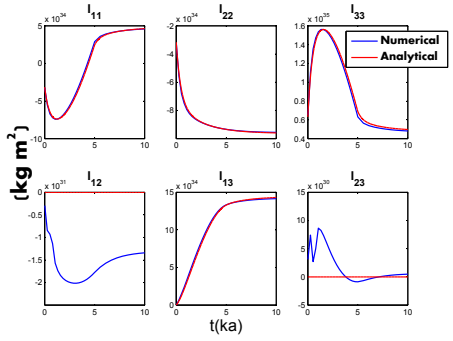

Figure 2: Change in moment of inertia for a two-layer Earth model with rotation axis linearly drifting from 0° to 45° within $x - z$ plane in 5 thousand years. The model is initially an unloaded sphere.

3 Conclusion

The governing equations for the polar wander are solved numerically and the change in the moment of inertia which is analytically calculated by Equation 1 can be obtained directly from a finite element model. Together, a numerical approach which can deal with laterally heterogeneous planet model is developed.

Acknowledgements

We would like to thank Hermes Jara Orue for the helpful discussion. This research has been financially supported by the GO program of the Netherlands Organization for Scientific Research (NWO).

References

[1] Yanick Ricard, Giorgio Spada, and Roberto Sabadini. Polar wandering of a dynamic earth. Geophysical Journal International, 113(2):284–298, 1993.

[2] P. Wu. Using commercial finite element packages for the study of earth deformations, sea levels and the state of stress. Geophysical Journal International, 158(2):401–408, 2004.

[3] Patrick Wu and W. R. Peltier. Pleistocene deglaciation and the earth's rotation: a new analysis. Geophysical Journal of the Royal Astronomical Society, 76(3):753–791, 1984.

EPSC Abstracts
Vol. 10, EPSC2015-48, 2015
European Planetary Science Congress 2015

Coupling giant impacts and long-term evolution models

G. J. Golabek (1,2), A. Emsenhuber (3), M. Jutzi (3), T. V. Gerya (2) and E. I. Asphaug (3)
(1) Bayerisches Geoinstitut, University of Bayreuth, Bayreuth, Germany, (2) Institute of Geophysics, ETH Zurich, Zurich, Switzerland, (3) Institute of Physics, University of Bern, Bern, Switzerland, (4) School of Earth and Space Exploration, Arizona State University, Tempe, AZ, USA (gregor.golabek@uni-bayreuth.de)

Abstract

The crustal dichotomy [1] is the dominant geological feature on planet Mars. The exogenic approach to the origin of the crustal dichotomy [2-6] assumes that the northern lowlands correspond to a giant impact basin formed after primordial crust formation. However these simulations only consider the impact phase without studying the long-term repercussions of such a collision.
The endogenic approach [7], suggesting a degree-1 mantle upwelling underneath the southern highlands [8-11], relies on a high Rayleigh number and a particular viscosity profile to form a low degree convective pattern within the geological constraints for the dichotomy formation. Such vigorous convection, however, results in continuous magmatic resurfacing, destroying the initially dichotomous crustal structure in the long-term.
A further option is a hybrid exogenic-endogenic approach [12-15], which proposes an impact-induced magma ocean and subsequent superplume in the southern hemisphere. However these models rely on simple scaling laws to impose the thermal effects of the collision.
Here we present the first results of impact simulations performed with a SPH code [16,17] serially coupled with geodynamical computations performed using the code I3VIS [18] to improve the latter approach and test it against observations. We are exploring collisions varying the impactor velocities, impact angles and target body properties, and are gauging the sensitivity to the handoff from SPH to I3VIS.
As expected, our first results indicate the formation of a transient hemispherical magma ocean in the impacted hemisphere, and the merging of the cores. We also find that impact angle and velocity have a strong effect on the post-impact temperature field [5] and on the timescale and nature of core merger.

References

[1] McCauley J. F., Carr M. H., Cutts J. A., Hartmann W. K., Masursky H., Milton D. J., Sharp R. P. and Wilhelms D. E., 1972. *Icarus* 17, 289-327.

[2] Wilhelms D. E. and Squyres S. W., 1984. *Nature* 309, 138-140.

[3] Frey H. and Schultz R. A., 1988. *Geophys. Res. Lett.* 15, 229-232.

[4] Andrews-Hanna J. C., Zuber M. T. and Banerdt W. B., 2008. *Nature* 453, 1212-1215.

[5] Marinova M. M., Aharonson O. and Asphaug E., 2008. *Nature* 453, 1216-1219.

[6] Nimmo F., Hart S. D., Korycansky D. G. and Agnor C. B., 2008. *Nature* 453, 1220-1223.

[7] Weinstein S. A., 1995. *J. Geophys. Res.* 100, 11719-11728.

[8] Zhong S. and Zuber M. T., 2001. *Earth Planet. Sci. Lett.* 189, 75-84.

[9] Roberts J. H. and Zhong S., 2006. *J. Geophys. Res.* 111, E06013.

[10] Zhong S., 2009. *Nature Geosci.* 2, 19-23.

[11] Keller T. and Tackley P. J., 2009. *Icarus* 202, 429-443.

[12] Reese C. C. and Solomatov V. S., 2006. *Icarus* 184, 102-120.

[13] Reese C. C. and Solomatov V. S., 2010. *Icarus* 207, 82-97.

[14] Reese C. C., Orth C. P. and Solomatov V. S., 2010. *J. Geophys. Res.* 115, E05004.

[15] Golabek G. J., Keller, T., Gerya, T. V., Zhu G., Tackley P. J. and Connolly J. A. D. 2011. *Icarus* 215, 346-357.

EPSC Abstracts
Vol. 10, EPSC2015-107, 2015
European Planetary Science Congress 2015

Giant impacts, heterogeneous mantle heating and a past hemispheric dynamo on Mars

J. Monteux (1), H. Amit (2), G. Choblet (2), B. Langlais (2) and G. Tobie (2)
(1) Laboratoire Magmas et Volcans, Université Blaise Pascal, CNRS, IRD, Clermont-Ferrand, France, (2) Laboratoire de Planétologie et de Géodynamique, CNRS, Nantes, France (j.monteux@opgc.univ-bpclermont.fr)

Abstract

The martian surface exhibits a strong dichotomy in elevation, crustal thickness and magnetization between the southern and northern hemispheres. A giant impact has been proposed as an explanation for the formation of the Northern Lowlands on Mars. Such an impact probably led to strong and deep mantle heating which may have had implications on the magnetic evolution of the planet. We model the effects of such an impact on the martian magnetic field by imposing an impact induced thermal heterogeneity, and the subsequent heat flux heterogeneity, on the martian core-mantle boundary (CMB). The CMB heat flux lateral variations as well as the reduction in the mean CMB heat flux are determined by the size and geographic location of the impactor. A polar impactor leads to a north-south hemispheric magnetic dichotomy that is stronger than an east-west dichotomy created by an equatorial impactor. The amplitude of the hemispheric magnetic dichotomy is mostly controlled by the horizontal Rayleigh number Ra_h which represents the vigor of the convection driven by the lateral variations of the CMB heat flux. We show that, for a given Ra_h, an impact induced CMB heat flux heterogeneity is more efficient than a synthetic degree-1 CMB heat flux heterogeneity in generating strong hemispheric magnetic dichotomies. Large Rah values are needed to get a dichotomy as strong as the observed one, favoring a reversing paleo-dynamo for Mars. Our results imply that an impactor radius of ~ 1000 km could have recorded the magnetic dichotomy observed in the martian crustal field only if very rapid post-impact magma cooling took place.

EPSC Abstracts
Vol. 10, EPSC2015-221, 2015
European Planetary Science Congress 2015

On the cooling of a deep terrestrial magma ocean

J. Monteux (1), D. Andrault (1), H. Samuel (2)
(1) Laboratoire Magmas et Volcans, Université Blaise Pascal, CNRS, IRD, Clermont-Ferrand, France,
(2) Institut de Recherche en Astrophysique et Planétologie, CNRS, Toulouse (j.monteux@opgc.univ-bpclermont.fr)

Abstract

We have developed numerical models to monitor the thermo-chemical evolution of a cooling and crystallizing magma ocean from an initially fully molten mantle. For this purpose, we use a 1D spherical approach accounting for turbulent convective heat transfer. Our numerical model benchmarked with analytical solutions solves the heat equation with extremely fine grid spacing (down to the mm), which is a strong requirement for resolving properly thin thermal boundary layers. This model also integrates recent and strong experimental constraints from mineral physics.

1 Introduction

During its early evolution, geochemical evidences suggest that the Earth's mantle has experienced several episodes of global melting leading to the formation of the early continental crust [1] or facilitating the core formation [2]. The late stages of planetary formation probably involved several large to giant impacts [3]. Although not yet clearly established, it is likely that these giant impacts, such as the one that probably formed the Earth-Moon system, could have melted 30 to 100% of the Earth's mantle depending on the impactor/target mass ratio and on the pre-impact thermal state of the target [4]. Hence, the likelihood of episodic fully molten mantle is important.

The dynamics of such a thick magma ocean is very turbulent because of the small viscosity of the fully molten mantle material [5]. Studies of the magma ocean cooling are often restricted to the first 1000-2000 km. The aim of our study is to characterize the cooling dynamics within a fully molten magma ocean. We explore different initial magma ocean thermal states as well as different initial core temperatures. Our model integrates recent and strong experimental constraints such as the melting curves (solidus and liquidus) that have been determined up to core-mantle boundary conditions [6]. Our model also benefits from the recent advances in the determination of the equation of state of silicate liquids and of the thermal conductivity of deep mantle material.

2 Numerical models

We model the secular cooling of a fully molten magma ocean by convective transport of heat in a 1-D spherically symmetric geometry. In vigorously convecting systems such as magma oceans, the temperature distribution is nearly adiabatic and isentropic [5]. Hence as the initial condition we assume an adiabatic temperature profile with a surface temperature of 3000 K. The solidus and liquidus may play a major role in the early thermal evolution of the magma ocean. Recent laboratory experiments now constrain the liquidus and solidus of chondritic material up to pressures compatible with the core mantle boundary conditions [6] (Fig.1).

Because of the low viscosity of the molten magma ocean, Rayleigh numbers can reach values ranging from 10^{20} to 10^{30} [5]. We model the thermal evolution of a deep magma ocean using a spherically symmetric one-dimensional single-phase flow model. We solve the following equation of heat transfer:

$$\rho C_p \frac{\partial T}{\partial t} = \nabla.(k\nabla T) + \rho H \qquad (1)$$

with ρ is the density, C_p is the mantle heat capacity, T is the temperature, t is the time, k is the thermal conductivity and H is the radiogenic heating.

Thermal energy is efficiently transferred by thermal convection in the region where the temperature gradient is steeper than the adiabatic temperature gradient. In Eq. 1, the thermal conductivity k is the sum of the intrinsic thermal conductivity of the mantle material k_c and the effective thermal conductivity due to thermal convection k_v. We estimate the effective thermal conductivity as follows [8]:

$$k_v = F_{conv} L / \Delta T$$

$$F_{conv} = 0.089 k_c \Delta T Ra^{1/3} / L \quad (2)$$

$$Ra = \frac{\alpha g(r) C_p \rho^2 \Delta T L^3}{k\eta}$$

where L is the thickness of the magma ocean, F_{conv} is the convective heat flux, ΔT is the temperature excess relative to the adiabatic temperature profile, Ra is the Rayleigh number, α is the thermal expansion coefficient of the magma ocean, $g(r)$ is the gravity at radius r and η is the local dynamic viscosity.

3 Results

Our preliminary results (Fig. 1) show that the temperature rapidly decreases down to the liquidus temperature of the mantle and solidification occurs first from the surface where the temperature is imposed to 273 K leading to the formation of a thin crust in the thermal boundary layer [5]. Then, solidification occurs at the bottom as the liquidus is steeper than the adiabatic temperature profile. The solid fraction increases up to a critical value separating the turbulent liquid regime from the solid-state viscous regime [5,7]. As soon as this critical value is reached (within $\sim$ 1000 yr) the efficiency of mantle cooling becomes limited.

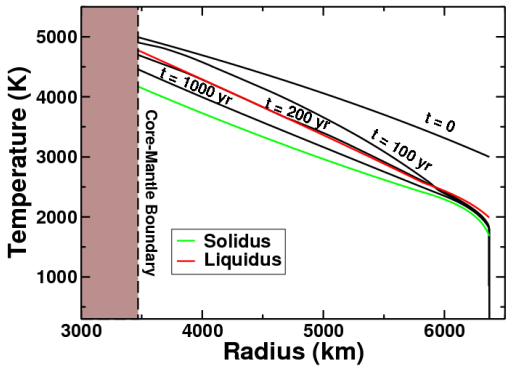

Figure 1: Preliminary calculations of the cooling of a fully molten Earth, using a 1D model to solve the heat equation at each depth.

4 Conclusion

We show that a deep magma ocean starts to cristallise rapidly after its formation. Then, once the melt fraction reaches a critical value, the cooling efficiency becomes limited. This decrease in the cooling rate can have important consequences for the deep thermal state of the mantle, the chemical fractionation of compatible/incompatible elements and, hence for the formation of a dense basal magma ocean [9].

Acknowledgments

J. Monteux and D. Andrault are funded by Agence Nationale de la Recherche (Oxydeep decision no. ANR-13-BS06-0008).

References

[1] Rizo, H., et al., Early mantle dynamics inferred from ^{142}Nd variations in Archean rocks from southwest Greenland. Earth Planet. Sci. Lett., 377, 324-335 (2013).

[2] Kleine, T., et al., Rapid accretion and early core formation on asteroids and the terrestrial planets from Hf-W chronometry. Nature, 418, 952-955 (2002).

[3] Agnor, C.B., et al., On the character and consequences of large impacts in the late stage of terrestrial planet formation. Icarus 142, 219-237 (1999).

[4] Canup, R., Lunar-forming impacts: processes and alternatives. PNAS, 374, 20130175 (2014)

[5] Solomatov, V.S., Magma oceans and primordial mantle differentiation. In: Schubert, G.(Ed.), Treatise on Geophysics, vol. 9, 91-120 (2007).

[6] Andrault, D. et al. Solidus and liquidus profiles of chondritic mantle : Implication for melting of the Earth across its history. Earth Planet. Sci. Lett., 304, 251-259 (2011).

[7] Abe, Y. Thermal and chemical evolution of the terrestrial magma ocean. Phys. Earth Planet. Int., 100, 27-39 (1997).

[8] Neumann, W., et al., Differentiation of Vesta: Implications for a shallow magma ocean, Earth Planet. Sci. Lett., 395, 267-280 (2014).

[9] Labrosse, S., et al., A crystallizing dense magma ocean at the base of the Earth's mantle. Nature, 450, 866-869 (2007)

EPSC Abstracts
Vol. 10, EPSC2015-300, 2015
European Planetary Science Congress 2015

Analysis of Curiosity surface temperature data

J. Audouard (1), S. Piqueux (2), F. Poulet (3), M. Vincendon (3) and B. Gondet (3)
(1) Stony Brook University, New York, USA, (2) Jet Propulsion Laboratory, California Insitute of Technology, Pasadena, California, USA, (3) Institut d'Astrophysique Spatiale, Université Paris Sud/CNRS, Orsay, France.
(joachim.audouard@stonybrook.edu)

Abstract

Since its landing in August 2012 in Gale crater, the rover Curiosity of the Mars Science Laboratory (MSL) NASA mission has performed many measurements to characterize its surroundings according to its science objectives [1]. In this work, we analyse the first year of data recorded by the Rover Environmental Monitoring Station (REMS) instrumental suite [2], and specifically by its Ground Temperature Sensor (GTS) which measures the temperature of the surface [3]. The temperature of the Martian surface is a complex function of the surface specific thermophysical properties (thermal inertia and albedo) and of the heterogeneity of the surface (horizontal mixing, and/or vertical heterogeneity, both expected on Mars). Using an Energy Balance model, we perform an analysis of GTS first year of data.

1. Introduction

The temperature of the Martian surface is a complex function of the surface specific thermophysical properties (thermal inertia and albedo) and of the heterogeneity of the surface (horizontal mixing, and/or vertical heterogeneity, both expected on Mars). When comparing surface temperature measure-ments with energy balance model predictions, it is possible to estimate the thermophysical properties of a surface. This method has been used by [4, 5, 6, 7] to infer the thermal inertia of the Martian surface using "single point" orbital surface temperature measure-ments. In the case of *in-situ* Curiosity surface temperature measurements, GTS/REMS data is recorded on a 1Hz sampling basis, for an average on-time of a few hours per sol. This unprecedented dataset thus allows for more refined thermophysical properties and regolith heterogeneity retrievals and can potentially reveal some processes which remain not accounted for in the energy balance models. This interest of GTS/REMS data has recently been emphazised by a couple of studies [8, 9], revealing that the GTS/REMS dataset effectively holds some information about processes influencing the temperature of Gale crater floor that remain to be understood.

We have performed an independent study of GTS/REMS surface temperature first Martian year of data using a different LMD-derived energy balance code and fitting method that those of [8, 9]. The purpose of this work is to retrieve the thermophysical properties of the regolith along Curiosity traverse, and to study and discriminate the non-simulated thermal behavior caused by regolith heterogeneities and neglected processes in the energy balance code.

2. Method

We identified a few hundred "stops" where Curiosity was still and GTS/REMS was turned on for at least a few hours. We use an Energy Balance Code derived from the LMD GCM [10] that was used for thermal inertia retrievals from orbital surface temperature data [7]. For each stop, there is a unique combination of thermal inertia and albedo that best fits GTS/REMS data in the least square sense. Data-resolution comparison between these best-fit surface temperature simulations and the actual data yield to a diurnal residual thermal behavior given the limitations of the surface temperature simulations (vertical and horizontal homogeneity) and the complexity of the real Martian regolith. Various processes un-accounted for in our model such as temperature-dependancy of the thermophysical properties [11] or the influence of the Curiosity nuclear power source are then added to the model, thus allowing an assessment of the different contributors to the observed thermal behavior. Comparison with orbital data will be presented.

3. Results

At first order, GTS/REMS data is well reproduced by the Energy Balance Code best fits.

Figure 1 shows an example where the residual ΔT is about 10 K throughout the sol over a total signal of ~100 K. The residual ΔT are surprinsigly stable throughout the mission (sol-to-sol as well as stop-to-stop), relatively independent of the location of the rover and of the thermophysical properties of its surroundings.

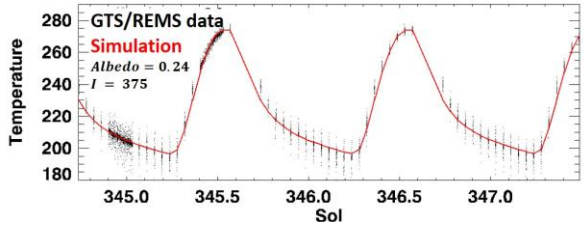

Figure 1. *Example of GTS/REMS surface temperature data and best fit simulation using an Energy balance code and the stated thermophysical properties.*

Figure 2 shows the average diurnal ΔT for the data corresponding to the four seasons and it can be seen that the non-accounted for thermal behavior is very regular: nighttime temperature measurements are always cooler that expected regarding the low daytime temperatures. Similarly, the morning heating happens to be really fast and the afternoon cooling is unexpectedly slow.

Deciphering the different contributors to this ΔT is ongoing, and first progress towards the integration and the impact of the temperature-dependency of thermal inertia are promising and will be presented and discussed at the conference.

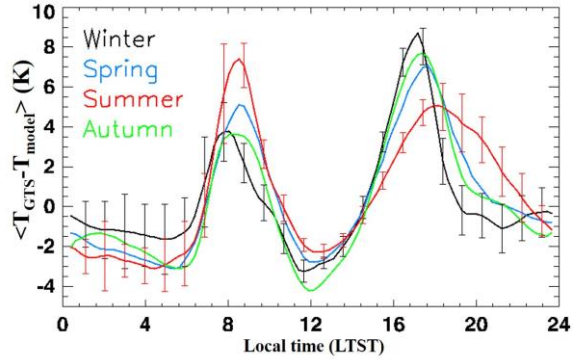

Figure 2. *Average residual ΔT (GTS minus best fit simulations) as a function of local time for the four seasons. Error bars represent the 3-sigma dispersion of the ΔT.*

A few K of the figure 2 thermal behaviour can be explained by this process. Additionnal T-dependant effects will be discussed.

We will also attempt to simulate the impact of the Curiosity nuclear power source by adding an energy input into the Energy Balance Model. Impact of mesoscale atmospheric processes (such as turbulences) will also be discussed. Our purpose is to estimate the impact of these different factors (T-dependancy of thermal inertia, impact of nuclear power source, mesoscale effect…) onto the GTS/REMS data in order to be left with a smaller ΔT that would be caused by the regolith thermophysical heterogeneities.

References

[1] Grotzinger, J. et al., Mars Science Laboratory Mission and Science Investigation, Space Science Reviews, vol. 170, pp. 5–56, 2012.

[2] Gómez-Elvira, J. et al., REMS : The Environmental Sensor Suite for the Mars Science Laboratory Rover, Space Science Reviews , vol. 170, pp. 583–640, 2012.

[3] Sebastián, E. et al., The Rover Environmental Monitoring Station Ground Temperature Sensor: A Pyrometer for Measuring Ground Temperature on Mars, Sensors, vol. 10, pp. 9211-9231, 2010.

[4] Kieffer, H. et al, Thermal and albedo mapping of Mars during the Viking primary mission, Journal of Geophysical Research, vol. 82, pp. 4249–4291, 1977.

[5] Mellon, M. et al., High-Resolution Thermal Inertia Mapping from the Mars Global Surveyor Thermal Emission Spectrometer, Icarus, vol. 148, 2000.

[6] Fergason, R. L. et al., High-resolution thermal inertia derived from the Thermal Emission Imaging System (THEMIS) : Thermal model and applications, Journal of Geophysical Research : Planets, vol. 111, 2006.

[7] Audouard, J. et al., Mars surface thermal inertia and heterogeneities from OMEGA/MEX, Icarus, vol. 233, pp. 194-213, 2014.

[8] Hamilton, V., et al, Observations and preliminary science results from the first 100 sols of MSL Rover Environmental Monitoring Station ground temperature sensor measurements at Gale Crater, Journal of Geophysical Research, vol. 119, pp. 745–770, 2014.

[9] Martinez, G. et al., Surface energy budget and thermal inertia at Gale Crater : Calculations from groundbased Measurements, Journal of Geophysical Research, vol. 119, 2014.

[10] Forget, F. et al., Improved general circulation models of the Martian atmosphere from the surface to above 80 km, Journal of Geophysical Research, vol. 104, pp. 24155–24175, 1999.

[11] Piqueux, S. and Christensen, P. R., Temperature-dependent thermal inertia of homogeneous Martian regolith, Journal of Geophysical Research, vol. 116, 2011.

EPSC Abstracts
Vol. 10, EPSC2015-511, 2015
European Planetary Science Congress 2015

A tracers method for studying double diffusive convection in the liquid layers of planetary interiors

M. Bouffard (1,2), S. Labrosse (1), G. Choblet (2), A. Fournier (3), J. Aubert (3) and P. Tackley (4)
(1) ENS Lyon, France, (2) LPG, Nantes, France, (3) IPG, Paris, France, (4) ETH, Zurich, Switerzland
(mathieu.bouffard@ens-lyon.fr)

Abstract

Convection in the liquid layers of planetary interiors is usually driven by a combination of thermal and compositional sources of buoyancy. The low molecular diffusivity of composition causes troubles in the description of this field on the Eulerian grids typically employed in current codes of geodynamo because numerical diffusion on these grids is potentially larger than the real diffusivity. We developed a Lagrangian description of composition based on a method of tracers. The absence of numerical diffusion inherent to this method allows modeling of thermo-chemical convection with infinite Lewis number. The validation of this new tool on benchmark cases will be presented at EPSC as well as its first applications to the ocean of Ganymede with consistently coupled boundary conditions for temperature and composition.

1. Introduction

The liquid part of planetary cores is assumed to be composed of a mixture of iron and nickel, plus a small fraction of light elements, probably sulphur, oxygen or silicon [7]. Convection in these layers is usually driven by the combination of two sources of buoyancy: a thermal source directly related to the planet's secular cooling, the release of latent heat and the heat generated by radioactive decay, and a compositional source due to some process of cristallisation, for example the growth of a solid inner core which releases light elements into the liquid outer core. The molecular diffusivity of composition is at least 3 orders of magnitude lower than that of temperature [1], which can produce differences in the dynamics inherent to thermal and compositional convection, respectively.

The classical approach that has been proposed by Braginsky and Roberts [1] and widely adopted since consists in combining both sources of buoyancy into a single component named codensity, under the assumption that the action of turbulence simply enhances the diffusivities of both fields to a same turbulent value. Codensity is a very convenient approach but it remains limited and simplistic. Firstly, it does not allow for a correct description of the distinct and coupled boundary conditions for temperature and composition. Secondly, due to the complexities of core turbulence which is probably anisotropic ([1],[6]), codensity turns out to be only a rough approximation and its use may be particularly problematic inside stratified layers ([6],[5]), in which it is likely that turbulence will be much less efficient if not absent, causing the mixing of properties being rather performed by molecular diffusion [1]. For a more rigorous description, one should therefore solve distinct transport equations for temperature and composition using two different diffusivities. This "double diffusivity" scenario has already been studied ([6],[2],[8]) but only through a limited exploration of the parameters space, the ratio of the thermal and chemical diffusivities, called the Lewis number $Le = \kappa_T/\kappa_C$, being kept below a value of 10 in these studies. The reason for this limitation is purely technical and closely related to the fact that describing physical variables on a Eulerian grid generates numerical diffusion, this latter being potentially larger than the actual molecular diffusivities and therefore hiding appropriate transport phenomena with low diffusivities. In this work, we developed a Lagrangian description of composition based on the introduction of tracers in a Eulerian grid. Such a method theoretically guarantees the absence of numerical diffusion.

2. Principle of the method

A Lagrangian method is used to solve the transport equation for composition C, in which $\mathbf{u}$ is the velocity and Pr_C the compositional Prandtl number:

$$\frac{\partial C}{\partial t} + \mathbf{u} \cdot \nabla C = \frac{1}{Pr_C} \nabla^2 C \qquad (1)$$

A large number of particles (tracers) are initially dispersed through the Eulerian grid. Each tracer contains

its coordinates and the value of composition at its position. At each time step, the tracers are advected by the flow via a 4th-order Runge Kutta scheme by interpolating the velocity from grid nodes to their positions. This interpolation is quadratic in the direction along which there are strong variations of the velocity gradient and linear in the other directions. In the vicinity of poles, tracers are advected in cartesian coordinates to avoid deformation due to the spherical geometry. After advection, the composition field is updated on each grid node by perfoming trilinear interpolation with the surrounding tracers. For the diffusive part, a subgrid scale diffusion operation is performed similarly to Gerya and Yuen, 2003 [4]. This method was implemented in the code PARODY (E. Dormy, J. Aubert) and parallelised using MPI and OpenMP, permitting to run simulations within reasonable time. Several advection tests were performed to check that this method does not produce numerical diffusion and will be shown at EPSC (fig. 1).

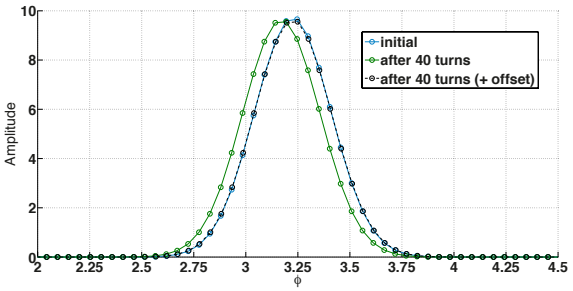

Figure 1: Profile of a gaussian equatorial patch before and after 40 turns of solid rotation around the equator. The shape has not changed confirming the absence of numerical diffusion during advection.

3. Benchmarking

In order to validate this method, we ran simulations on the benchmark case 1 proposed by Christensen et al., 2001 [3]. In this test, tracers are used to solve the transport equation for temperature. Note that since the gain with tracers resides mainly in the ability to treat low-diffusive fields, not in some improvement of the code's precision, we only need the results to be in correct agreement with the benchmark's standard solution. Preliminary results are given in table 1 and show sufficient agreement even at low resolution. Runs at higher resolution will be shown at EPSC as well as results on the thermo-chemical benchmark proposed by Breuer et al., 2010 [2].

Table 1: Preliminary benchmark case 1 results at low resolution ($N_r = 90, N_\theta = 66, l_{max} = 44$), with (Parody^{tra}) and without tracers (Parody). See [3] for the terms definitions.

	Standard	Parody	Parody^{tra}
E_{kin}	30.733	30.964	30.271
E_{mag}	626.41	629.27	623.70
T	0.37338	0.3730	0.3729
u_ϕ	-7.6250	-7.3465	-7.2855
B_θ	-4.9289	-4.9934	-4.9499
ω	-3.1017	-3.1200	-2.9960

4. Applications

Our present focus is to implement thermodynamically consistently coupled boundary conditions for temperature and composition. In a first step, we intend to apply this new tool to non-magnetic thermo-chemical convection in the ocean of Ganymede. The results obtained will be presented at EPSC.

Acknowledgements

Numerical simulations were performed on three different platforms at IDRIS, Orsay, CCIPL, Nantes and PSMN, Lyon, France. We also thank Guy Moebs and Cerasela Iliana Calugaru for technical support. This work also benefited from helpful discussions with Hagay Amit and Philippe Cardin.

References

[1] Braginsky and Roberts, *Geophys. Astrophy. Fluid Dynamics*, *79*, 1–97.

[2] Breuer et al., *Geophys. J. Int.*, *183*, 150–162.

[3] Christensen et al., *Phys. Earth Planet. Inter.*, *128*, 25–34.

[4] Gerya and Yuen, *Phys. Earth Planet. Inter.*, *140*, 293–318.

[5] Gomi et al., *Phys. Earth Planet. Inter.*, *224*, 88–103.

[6] Manglik et al., *Earth Planet. Sci. Lett.*, *289*, 619–628.

[7] Poirier, J. P., *Earth Planet. Sci. Inter.*, *85*, 319–337

[8] Trümper et al., *Phys. Earth Planet. Inter.*, *194–195*, 55–63.

EPSC Abstracts
Vol. 10, EPSC2015-654, 2015
European Planetary Science Congress 2015

Geophysical Limitations on the Habitable Zone

L. Noack and T. Van Hoolst
Royal Observatory of Belgium, Belgium (lena.noack@oma.be)

Abstract

Planets are typically classified as potentially life-bearing planets (i.e. habitable planets) if they are rocky planets and if a liquid (e.g. water) could exist at the surface. The latter depends on several factors, like for example the amount of available solar energy, greenhouse effects in the atmosphere and an efficient CO_2-cycle. However, the definition of the habitable zone should be updated to include possible geophysical constraints, that could potentially influence the CO_2-cycle. Planets like Mars without plate tectonics and no or only limited volcanic events can only be considered to be habitable at the inner boundary of the habitable zone, since the greenhouse effect needed to ensure liquid surface water farther away from the sun is strongly reduced. We investigate how these geophysical processes depend on the mass and interior structure of terrestrial planets. We find that plate tectonics, if it occurs, always leads to sufficient volcanic outgassing and therefore greenhouse effect needed for the outer boundary of the habitable zone (several tens of bar CO_2). One-plate planets, however, may suffer strong volcanic limitations if their mass and/or iron content exceeds a critical value, reducing their possible surface habitability.

1. Introduction

The well-known circumstellar habitable zone (HZ) gives the distance to a star where liquid water may exist for a terrestrial planet. It assumes a fixed Earth-like CO2-cycle including the life-enhanced carbon-silicate cycle, active volcanism and plate tectonics, which are needed to regulate the atmosphere via the amount of outgassed greenhouse gases or subducted carbonates. The concept of the HZ, however, neglects the possible planetary diversity that we can already see in the Solar System. The Earth is only one out of three planets in the HZ - with Mars and Venus at the boundaries. Both those planets lack plate tectonics, a global magnetic field and (at least in the case of Mars) active volcanism. The planet mass as well as the interior structure can set constraints on the occurrence of plate tectonics and outgassing, and therefore affect the habitable zone.

2. Geophysical modeling

In order to understand how the interior of a planet may influence its potential surface habitability, we apply two numerical convection codes – CHIC [1] and GAIA [2]. We investigate how the mass and interior structure of terrestrial planets may influence the outgassing efficiency as well as the likelihood to form long-term plate tectonics.

We use an interior structure model (included in CHIC) to obtain profiles for the depth-dependent pressure and gravity acceleration. The density, the thermal expansion coefficient and the heat capacity at local conditions are obtained from equations of states of the relevant materials [1]. For the simulation of plate tectonics, a 2D convection code is used to investigate local stresses. Plastic deformation occurs if these stresses exceed the local, material-dependent yield stress. For the volcanic outgassing, we model the formation of partial melt in the mantle both with a 1D parameterized model (CHIC) as well as with 2D convection simulations (both codes).

3. Results

3.1 Plate tectonics depending on interior

Plate tectonics has an important influence on partial melting and thus volcanism since the melting temperature depends on the pressure. Upwelling of hot mantle material to the surface (e.g., at mid-ocean ridges) leads to large amount of melting and outgassing [3].

First, we investigate the possible initiation of plate tectonics for Earth-sized planets of different masses and thus compositions. We find that plate tectonics is less likely to occur for planets with a small core or a very large, Mercury-like core [3]. In the intermediate regime (with cores slightly larger than Earth's core), a long-wavelength convection structure occurs, that leads to larger stresses at the bottom of the lithosphere and enhanced plastic deformation.

Besides the core size, the mass of the planet also plays a crucial role for initiation of plate tectonics. For small bodies as Mars, our simulations suggest that long-term plate tectonics is unlikely without large tidal heating effects or unrealistic high amounts of radioactive heating, even though very short term lithosphere mobilization in the beginning of the thermal evolution cannot entirely be ruled out. Large super-Earths on the other hand may experience the opposite problem: too strong convection or too high radioactive heating can favor stagnant lid convection over plate tectonics, whereas cooler super-Earths may form an almost stagnant lower mantle due to the effect pressure has on the viscosity [4].

3.4 Outgassing depending on interior

For stagnant lid planets, outgassing is strongly limited if the pressure in the upper-most part of the mantle is large enough such that the melting temperatures are above the adiabatic mantle temperature. These large pressures can occur for either large iron cores (since iron is denser than silicates, influencing the surface gravity and thus pressure [3]), or for high planet masses, as shown in Figure 1 (using the 2D convection code GAIA). Note that if plate tectonics occurs, hot mantle material can reach the surface, leading to pressure-release melting.

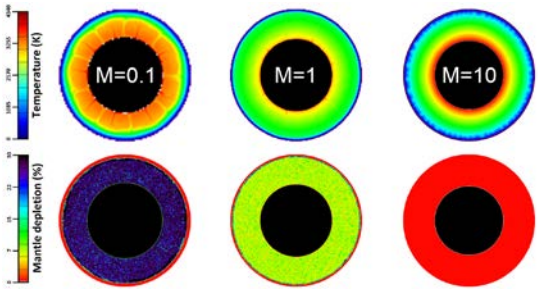

Figure 1: Temperature field and melt depletion after 4.5 Gyr for an Earth-like interior structure but different planet masses (neglecting possible plate tectonics) or mass and interior structure (right).

We use a 1D parameterized model (CHIC, [1]) to investigate how melting depends on both planet mass and interior structure, see Figure 2. We observe that the depletion of the mantle and thus the outgassing efficiency is strongly reduced for increasing planet mass (with zero outgassing from a critical mass and critical interior structure on). Depletion is also strongly reduced for increasing iron content and thus core sizes.

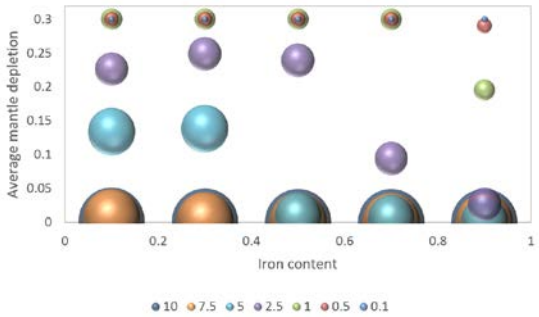

Figure 2: Average mantle depletion depending mass and iron content (i.e. iron core size).

Note, that the critical mass and iron content, from which on no depletion can be observed anymore, depends strongly on the initial mantle temperature. The amount of radioactive heat sources as well as a possible heat source enrichment in the (possibly primordial) crust could also influence the observed critical values.

4. Summary and Conclusions

The existence of a dense-enough CO_2 atmosphere allowing for the carbon-silicate cycle and release of carbon at the outer boundary of the habitable zone may be strongly limited for planets: 1) without plate tectonics, 2) with a large planet mass, and/or 3) a high iron content.

Acknowledgements

This work has been funded by the Interuniversity Attraction Poles Programme initiated by the Belgian Science Policy Office through the Planet Topers alliance, and results within the collaboration of the COST Action TD 1308.

References

[1] Noack, L., Rivoldini, A., and Van Hoolst, T.: CHIC – Coupling Habitability, Interior and Crust, Conference paper, INFOCOMP 2015, Brussels, Belgium.

[2] Hüttig, C. and Stemmer, K.: Finite volume discretization for dynamic viscosities on Voronoi grids, PEPI, Vol 171, pp. 137-146, 2008.

[3] Noack, L. et al.: Constraints for planetary habitability from interior modeling, PSS, Vol. 98, pp. 14-29, 2014.

[3] Noack, L., and Breuer, D.: Plate tectonics on rocky exoplanets: Influence of initial conditions and mantle rheology, PSS, Vol. 98, pp. 41-49, 2014.

EPSC Abstracts
Vol. 10, EPSC2015-681, 2015
European Planetary Science Congress 2015

Effect of width, amplitude and position of a CMB hot spot on core convection and dynamo action

W. Dietrich (1), K. Hori (1) and J. Wicht (2)
(1) Department of Applied Mathematics, University of Leeds, Leeds, UK (2) Max Planck Insitute for Solar System Research, Göttingen, Germany (w.dietrich@leeds.ac.uk)

Abstract

Within the fluid iron cores of terrestrial planets, convection and hence the generation of global magnetic fields are controlled by the overlying rocky mantle. The thermal structure of the lower mantle determines how much heat is allowed to escape the core. Hot lower mantle features, like the thermal footprint of a giant impact or hot mantle plumes will reduce locally the heat flux through the core mantle boundary (CMB) and thereby weaken core convection and affect the magnetic field generation process. In this study, we numerically investigate how parametrised hot spots at the CMB with arbitrary size, amplitude and position affect core convection and hence the dynamo. The effect of the heat flux anomaly is quantified by changes in global flow symmetry properties, such as the emergence of equatorial antisymmetric and axisymmetric (EAA) zonal flows. For pure hydrodynamic models the EAA symmetry scales almost linearly with its respective amplitude and size, whereas self-consistent dynamo simulations typically either suppress or drastically enhance EAA depending mainly on the length scale of the heat flux anomaly. Our results suggest, that the horizontal extent of the anomaly should be on the order of the outer core radius to significantly affect flow and field symmetries. As an implication to Mars, the study concludes that an ancient core field modified by a CMB heat flux anomaly is not able to heterogeneously magnetise the crust to the present-day level of north-south asymmetry.

1. Introduction

The three terrestrial planets, Earth, Mercury and Mars harbour or once harboured a dynamo process in the liquid part of the iron-rich core. Vigorous core convection shaped by rapid planetary rotation is responsible for the generation of global magnetic fields. In terrestrial planets the amount of heat escaping the core is set by the thermal structure of the overlying mantle convection. As the vigorous core convection assures efficient mixing and hence a virtually homogeneous temperature at the core side of the CMB T_{core}, the flux through the CMB is entirely controlled by the lower mantle temperature T_{lm}, hence

$$q_{cmb} = k\frac{T_{lm} - T_{core}}{\delta_{cmb}} \,, \qquad (1)$$

where δ_{cmb} is the vertical thickness of the thermal boundary layer on the mantle side and k the thermal conductivity. Hot mantle features like convective upwellings, thermal 'footprints' of giant impacts or chemical heterogeneities locally reduce the heat flux rate through the CMB. E.g. for the planet Mars, low degree mantle convection or giant impacts might have significantly affected the core convection and the morphology of the induced magnetic field. The strong (south-)hemispherical preference of the crustal magnetisation can for example be explained by an ancient dynamo which operated more efficiently in the southern hemisphere [1]. Indeed, turned out that dynamo models obeying magnetic fields, which show a geometrically corresponding intensity distribution (hemispherical fields) are typically oscillatory and hence can not explain the thick and unidirectional magnetisation on Mars [2].

However these numerical models relied on a rather simplistic of the variation of the CMB heat flux as a single, large scale spherical harmonic (Y_{10}) was used. We therefore test the robustness of pessimistic models of the ancient Martian core with using a complex heat flux anomaly of variable width, amplitude and position.

2. Results

The main effect of the large-scale thermal anomaly is to introduce a global asymmetry on the mean temperature by reducing the heat flux in the northern and increasing it in the south. Mean flows seeking the equilibrate this temperature asymmetry are diverted into

azimuthal directions by the dominating thermal wind:

$$\frac{\partial \overline{u_\phi}}{\partial z} = \frac{RaE}{2Pr}\frac{1}{r_{cmb}}\frac{\partial \overline{T}}{\partial \theta}\,, \qquad (2)$$

where the colder (southern) hemisphere obeys much stronger convection and hence magnetic field induction (see figure 1).

Our results suggest that the fundamental temperature asymmetry developes independent of the anomaly width and position, a surprising result. Further we can show, that in hydrodynamic simulations without a magnetic field the relative strength of EAA-symmetric flows scales almost linearly with its respective amplitude and width, whereas in dynamo simulations the magnetic field either suppresses antisymmetric flows when weaker amomalies are applied or drastically enhances them for the stronger anomalies. We clearly identify and quantify the action of the magnetic field on the asymmetry of flow and temperature. Further we show that also smaller and weaker anomalies do not yield a hemispherical magnetic field what is both, stable in time and hemispherical enough.

3. Summary and Conclusions

Our numerical investigation of a planetary dynamo model subject to heterogeneous CMB heat flux, indicates three main conclusions. It turned out, that the fundamental temperature asymmetry driving equatorial antisymmetric and axisymmetric flows (EAA) emerges independent of the width, amplitude and position of the CMB hot spot. However, including the action of the induced magnetic field, we state that the horizontal extent of a CMB heat flux anomaly needs to exceed the radius of the core to affect core convection and magnetic field induction significantly. Finally as an implication to Mars, we conclude the hemispherical distribution of the present-day crust can not exclusively explained by an ancient core dynamo inducing a hemispherical magnetic field [3].

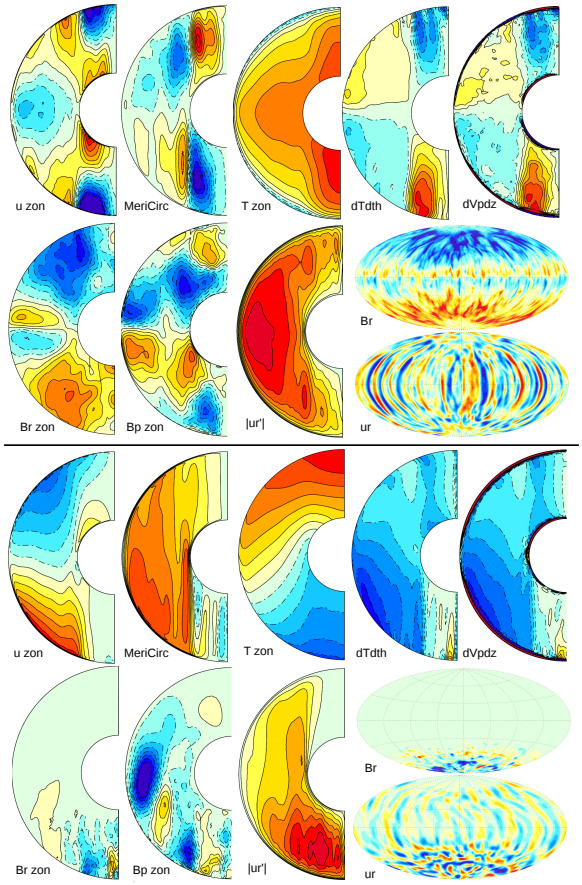

Figure 1: Mean flow and field properties for a case of homogeneous outer boundary heat flux (top part) and when a Y_{10}- heat flux anomaly is added (lower part).

References

[1] Stanley, S., Elkins-Tanton, L., Zuber, M.T. and Parmentier, E.M.: Mars' Paleomagnetic Field as the Result of a Single-Hemisphere Dynamo, Science, Vol. 321, 2008.

[2] Dietrich, W. and Wicht, J.: A hemispherical dynamo model: Implications for the Martian crustal magnetization, Physics of the Earth and Planetary Interiors, 217, 2013

[3] Dietrich, W., Wicht, J. and Hori, K.: Effect of width, amplitude and position of a CMB hot spot on core convection and dynamo action, under review at Progress in Earth and Planetary Sciences, 2015

EPSC Abstracts
Vol. 10, EPSC2015-774, 2015
European Planetary Science Congress 2015

2D dynamic model of convection dynamics in a complex ice mantle.

Effect of solid/solid phase transition on the chemical exchanges and the habitability of ocean planets.

B. Journaux (1) and L. Noack (2)
(1) Laboratoire de Glaciologie et Géophysique de l'Environnement, Grenoble, France (Baptiste.Journaux@lgge.obs.ujf-grenoble.fr), (2) Royal Observatory of Belgium, Belgium

Abstract

We model the possible material transport through high-pressure ice layers in water-rich planets. The model focusses on the influence of phase transitions on the convective patterns, where we apply physical properties of high pressure ice. We investigate if (or under which circumstances) the transport path through the ice may be blocked by phase-transition-induced multi-layer convection in the high-pressure ice layer.

1. Introduction

H_2O is one of the most abundant molecules in our galaxy and is present in a large variety of planetary environments [1,2]. In the last few years an increasing number of exoplanet discoveries suggested the existence of a new kind of planetary bodies very rich in H_2O that explain the low density of some relatively small planets [3].

They may contain a large H_2O-based icy mantle, up to thousands of kilometers thick, possibly overlaid by a liquid ocean. With such thermodynamic conditions the solid mantle would be dominated by dense high pressure ice polymorph, stable beyond the gigapascal (i.e. ice VI, ice VII or ice X) [2,4,5]. This thick ice mantle may represent a physical barrier for chemical exchange between the rocky core and the uppermost ocean. This is why the ocean of such planets are regarded as bad candidates for hosting habitable environment that would require inputs of nutrients.

Recent experimental results have suggested that a very different scenario might occur as some chemical species (e.g. NaCl, LiCl, RbI, CH_3OH) are soluble up to several mol% inside high pressure ice [6,7,8]. This would permit to bring nutrients to the ocean through solid-state convection [3,8]. A major limitation for such scenario is possible phase transitions inside the ice mantle that would imply viscosity, thermal physical properties and chemical solubility contrasts. This could alter convective currents and limit the possibility of upwarding solute flux and therefore the potential habitability of the uppermost ocean.

In the present work we study the influence of the presence of a phase transition on the convective patterns in a convective layer.

2. Modeling

We apply a Fortran convection codes (CHIC [9]) to investigate the convective behavior in a high-pressure ice layer including phase transitions. The density, the thermal expansion coefficient and the heat capacity at local conditions are obtained from equations of states of the relevant materials [9].

In our first simulations, we simulate a 200km deep high-pressure ice layer, where we apply a surface pressure of 1 GPa and a surface temperature of 280 K, leading to high-pressure ice phases VI and VII. The initial temperature profile is either constant or adiabatic. At the bottom, a temperature jump of 30 K acts as a heating source from below.

The density is determined self-consistently with local pressure and temperature after [10], heat capacity and thermal expansivity of ice phases VI and VII are taken from [10,11].
For our preliminary investigations, we apply a Newtonian viscosity law and ice VI rheology for the entire investigated high-pressure ice layer. Note that we use an increased reference viscosity (by a factor of 100) and neglect a possible pressure influence. The parameters for the rheology and for the phase transitions are listed in Table 1. The phase density jump is determined locally from the density profiles.

Table 1: Rheology and phase transition parameters

Parameter	Ice VI/VII
Activation energy [kJ/mol]	136
Reference viscosity [Pas]	$1 \cdot 10^{14}$
Reference temperature [K]	330
Phase transition pressure [GPa]	2.14
Phase transition temperature [K]	300
Clapeyron slope [MPa/K]	1.25

3. Results

Figure 1 shows the temperature field for a constant initial temperature profile in the ice layer. A two-layer convection pattern evolves, which strongly reduces material transport between the two layers.

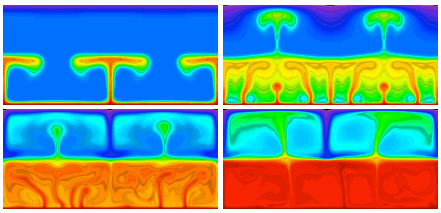

Figure 1: Temperature field at 1, 3, 6 and 13 Myr

For an initial adiabatic temperature profile, results are similar. With time, the ice VII layer heats up, as material transport through the phase boundary is again reduced due to the large density jump, see Fig. 2. At the start of the simulation, we put black and red tracers at the top and bottom of the investigated domain, to see if material exchange between the two high-pressure ice layers is possible.

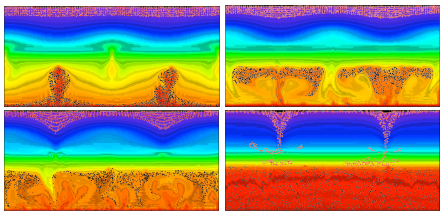

Figure 2: Temperature field including material tracers 0.05, 0.4, 1.3 and 11 Myr

In the lower half of the domain, strong convection leads to a homogeneous mixing in the ice VII layer. In the ice VI layer, convection acts on a longer time scale due to the colder temperatures, dominated by two downwellings, that are stopped at the ice VI-VII phase boundary. After 11 Myr, a small number of red particles can be found in the lithosphere of the ice VII layer, but no black tracers are in the ice VI layer.

4. Summary and Conclusions

Our first results show that the temperature profile, especially a possible temperature contrast at the bottom due to heating from the mantle below, has a major influence on the evolving convection pattern. More investigations including self-consistent thermodynamic profiles and inclusion of chemical species as well as melting processes will add to the picture.

Acknowledgements

B. Journaux is currently supported by the ANR-funded DREAM project on the plasticity of anisotropic material, awarded to M. Montagnat (LGGE – UMR 5183- UJF, Grenoble). L. Noack has been funded by the Interuniversity Attraction Poles Programme initiated by the Belgian Science Policy Office through the Planet Topers alliance.

References

[1] Cernicharo, J., Crovisier, J., 2005. Water in space: the water world of ISO. Space Sci. Rev. 119, 29–69.

[2] Fu, R., O'Connell, R., Sasselov, D., 2010. The Interior Dynamics of Water Planets. Astrophys. J. 708, 1326–1334.

[3] Léger, A., Selsis, F., Sotin, C., Guillot, T., Despois, D., Mawet, D., Ollivier, M., Labèque, A., Valette, C., Brachet, F., 2004. A new family of planets? Icarus 169, 499–504.

[4] Sotin, C., Grasset, O., 2007. Mass-radius curve for extrasolar Earth-like planets and ocean planets. Icarus 191, 337–351.

[5] Journaux, B., Caracas, R., Carrez, P., Gouriet, K., Cordier, P., Daniel, I., 2014. Elasticity and dislocations in ice X under pressure. Phys. Earth Planet. Inter. 236, 10–15.

[6] Klotz, S., Bove, L., Strässle, T., Hansen, T., Saitta, A., 2009. The preparation and structure of salty ice VII under pressure. Nat. Mater. 8, 405–409.

[7] Frank, M.R., Aarestad, E., Scott, H.P., Prakapenka, V.B., 2013. A comparison of ice VII formed in the H2O, NaCl-H2O, and CH3OH-H2O systems: Implications for H2O-rich planets. Phys. Earth Planet. Inter. 215, 12–20.

[8] Journaux, B., Daniel, I., Petitgirard, S., Cardon, H., Perrillat, J-P., Caracas, R., Mezouar, M, in prep. Salt partitioning at high-pressure between aqueous solution, ice VI and ice VII. Implication for water-rich planetary bodies dynamics and habitability.

[9] Noack, L., Rivoldini, A., and Van Hoolst, T.: CHIC – Coupling Habitability, Interior and Crust, Conference paper, INFOCOMP 2015, Brussels, Belgium.

[10] Bezacier, L., Journaux, B., Perrillat, J-P, Cardon, H., Hanfland, M., Daniel, I., 2014. Equations of state of ice VI and ice VII at high pressure and high temperature. J. Chem. Phys. 141, 104505.

[11] Tchijov, V., 2004. Heat capacity of high-pressure ice polymorphs. J. Phys. Chem. Solids 65, 851–854.

EPSC Abstracts
Vol. 10, EPSC2015-823, 2015
European Planetary Science Congress 2015

Influence of initial CO_2 content on a planet surface conditions at the end of the magma ocean phase

A. Salvador (1,2), H. Massol (2), A. Davaille (1), E. Marcq (3), P. Sarda (2), and E. Chassefière (2)
(1) FAST, CNRS/Univ. Paris-Sud, France, (2) GEOPS, CNRS/Univ. Paris-Sud, France, (3) LATMOS, CNRS/Univ. of Versailles St-Quentin, France (arnaud.salvador@u-psud.fr)

Abstract

The earliest compositional differentiation of the terrestrial planets, the formation of their outgassed atmospheres, and the existence of condensed water oceans over their solid mantles, are conditioned by magma ocean (MO) formation and solidification. Recent studies have suggested that depending on the planet initial water content and its orbital distance to the sun, two types of conditions, with (I) or without (II) water ocean, can prevail at the end of the MO phase. We use a coupled interior-atmosphere model of MO thermal evolution to go further and study systematically the influence of the planet initial CO_2 content on the resulting surface conditions (temperature, volatiles, condensed water) at the end of the MO phase. The position of the boundary between the two regimes is shown to depend also on the initial CO2 content.

1. Introduction

Conditions at the end of the magma ocean stage are important to constrain the subsequent evolution of a planet. Indeed, the resulting interior compositional structure constrains the geodynamical regime of a rocky planet and the resulting surface conditions determine the possibility of water condensation. Those conditions are therefore essential to determine the habitability of a planet and its temporal evolution.

Hamano & al. [1] demonstrated that the initial H_2O content of magma oceans has a significant influence on planetary evolution, leading to two different types of planetary surface condition as a function of the orbital distance from the sun. Here we decided to test specifically the influence of the initial CO_2 concentration on the surface condition at the end of the magma ocean phase.

2. Method

We used a 1-D parameterized convection model of a magma ocean coupled with a 1-D radiative-convective model of the atmosphere (Lebrun et al, 2013 [1]). The entire mantle of the planet is assumed to have melted, following collision with a giant impactor. The resulting MO is convecting at very high Rayleigh number and crystallizes from the bottom up. The magma viscosity depends on both temperature and crystal content. A rheological transition with a sharp increase in viscosity happens when the crystals volume fraction becomes greater than 60%. The end of the MO phase is defined as the time when this rheological front reaches the surface.

The 1-D radiative-convective atmospheric model (Marcq, 2012, [3]) considers an H_2O-CO_2 atmosphere which follows a vertical temperature profile similar to Kasting (1988) and Abe and Matsui (1988). Opacities in the thermal IR are computed using a k-correlated code (KSPECTRUM). The reflectance of the clouds of this non-gray model can be varied, as well as the orbital distance from the sun.

The MO interior and the atmosphere are coupled through the balance of the atmospheric heat flux at the surface with the convective heat flux out of the mantle. Furthermore, the atmospheric model takes into account the exsolved volatiles from the magma ocean as the cooling progresses, and the mass fraction of dissolved volatiles in the MO is assumed to be in equilibrium with the atmospheric volatile content at each time step, due to vigorous convective movements in the liquid MO.

3. Results

Figure 1 below shows, for a given initial H_2O concentration ($4{,}3.10^{-2}$Wt% ~ $2M_{EarthOcean}$), the thermal evolution of the magma ocean for a type I planet at 1 AU (red curves) and for a type II planet at 0.63 AU (blue curves), without CO_2. The differences between the two types of planets appear clearly: whereas the solidification time of the type I planet is less than 1 Myr, the type II planet isn't cooled after ten Myr with a non-gray atmosphere. By varying the initial CO_2 content, we've seen that those times are only affected by 30% at most.

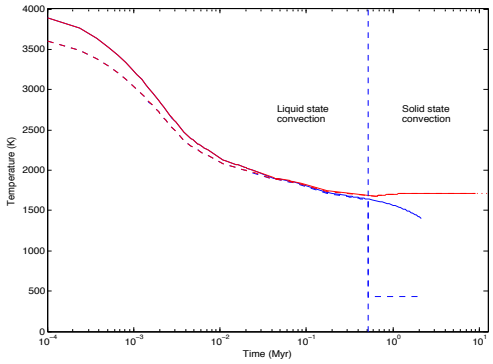

Figure 1: Evolution of the surface (dashed lines) and potential temperatures for type I (blue curves, 1.00 AU) and type II planets (red curves, 0.63 AU), with an initial water mass of twice the current oceans mass on Earth. These cases without CO_2 but a non-gray atmosphere compare well with Hamano et al's study.

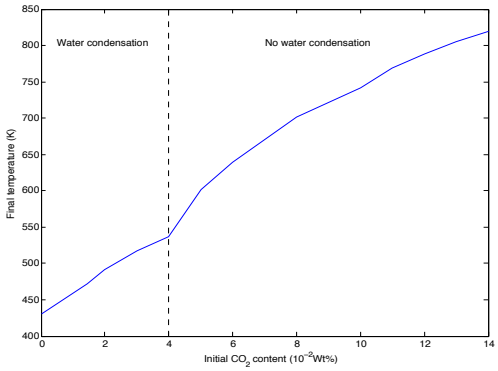

Figure 2: Surface temperature at the end of the magma ocean as a function of the initial CO_2 content for a solar distance of 1 AU, initial H_2O content equivalent to 0.6 current Earth's oceans, non-gray atmosphere.

Figure 2 shows the strong influence of the initial CO_2 content on the surface temperature obtained at the end of the magma ocean. It reveals the existence of two regimes, where the water condensation occurs or not and demonstrates that the initial CO_2 content of a planet must be taken into account to understand the evolution of a planet and especially its surface conditions. Thanks to those results, we can constrain the initial CO_2 content of a magma ocean for a given initial H_2O content for a planet where water condensed or not.

4. Conclusions

Using a combined atmosphere-MO evolution model, we showed that the initial CO_2 content significantly affects the surface conditions at the end of the magma ocean stage. For example, water condensation, depending on the surface temperature and pressure, can not occur above an initial CO_2 content of 4.10^{-2}wt% for a distance of 1 AU from the Sun with an initial H_2O content equivalent to 0.6 current Earth's oceans, in a non-gray atmosphere for an Earth-like planet. Thus, depending on the initial volatile content at the accretion time, it affects the habitability of a planet. However, this parameter doesn't affect significantly the solidification time of magma oceans. The model will also allow us to constrain the initial parameters that induce condensation such as the distance from the star and the initial CO_2 content for a given initial H_2O content. This model should be also applicable for exoplanets.

References

[1] Hamano, K., Abe, Y., and Genda, H.: Emergence of two types of terrestrial planet on solidification of magma ocean, Nature, Vol. 497, pp. 607-610, 2013.

[2] Lebrun, T. & al.: Thermal evolution of an early magma ocean in interaction with the atmosphere, Journal of Geophysical Research: Planets, Vol. 118, 2013.

[3] Marcq, E.: A simple 1-D radiative-convective atmospheric model designed for integration into coupled models of magma ocean planets, Journal of Geophysical Research: Planets, Vol. 117, 2012.